THE ELECTROMAGNETICALLY FORCED FLOW OVER A BACKWARD-FACING STEP

Tom Weier, Thomas Albrecht, Gunter Gerbeth
Department of Magnetohydrodynamics
Helmholtz-Zentrum Dresden-Rossendorf
Bautzner Landstr. 400, 01328 Dresden, Germany
{t.weier,t.albrecht,g.gerbeth}@hzdr.de

Sebastian Wittwer, Hans Metzkes, Jörg Stiller
Institut für Strömungsmechanik
Technische Universität Dresden
01062 Dresden, Germany
{sebastian.wittwer@mailbox.,hans.metzkes@,joerg.stiller@}tu-dresden.de

ABSTRACT

The flow over a backward-facing step is a prototype of a separating and reattaching shear flow and has therefore received a considerable amount of interest. We focus here on the excitation of the separated shear layer since it is often understood as the basic mechanism in active flow control. Forcing frequencies and amplitudes are obviously major parameters of influence, but different signal forms can have a profound impact as well, albeit the physical mechanism behind the latter is still not fully understood in the case of airfoils.

Electromagnetic body forces offer a simple and direct way to provide excitation by different wave forms. Particle image velocimetry measurements have been performed in a free surface electrolyte channel. We will discuss spatial amplification rates in the unforced shear layer, which show a fair agreement with results obtained by others in free shear layers. Compared to the natural flow, forcing near the optimal excitation frequency $St_{e\theta} = 0.012$ leads to a much earlier vortex roll-up and, consequently, the reattachment length is reduced. For the first subharmonic of the optimal excitation frequency, vortex roll up starts later but produces larger vortices. Excitation with the relatively high frequency of $St_{e\theta} = 0.03$ has only a very small effect on the flow. Keeping the excitation frequency at $St_{e\theta} = 0.012$ and increasing the forcing amplitude leads to earlier vortex roll up, larger vortices, and shorter reattachment lengths.

Using different wave forms to excite the shear layer at the most amplified frequency, the reattachment length is determined by the amplitude of the fundamental only.

INTRODUCTION

The flow over a backward-facing step is a prototype of a separating and reattaching shear flow and has received a considerable amount of interest since, as Roos & Kegelmann (1986) put it, "the process of shear-layer separation and reattachment is a key feature of many aerodynamic flow problems." Eaton & Johnston (1981) reviewed the earlier work on the flow developing under different geometrical settings. Bhattacharjee *et al.* (1986) and Roos & Kegelmann (1986) reported first results on backward-facing step flows under forcing by acoustic and electromechanical means. Many investigations on freely developing and forced flows over backward-facing steps have been published since, among which Huppertz (2001) provides a comprehensive account of the aspects of active control.

Our interest in the subject is founded in active flow control of stalled airfoils. Shear layer excitation is often understood as the basic mechanism in active flow control (Greenblatt & Wygnanski, 2000), but the separated flow on a stalled airfoil is quite complex. In the case of a stalled foil, the wake exerts a large influence on the flow dynamics. Moving separation points and strong three-dimensional effects further complicate the matter. Forcing frequencies and amplitudes are obviously major parameters in active flow control, but signal forms can be of influence as well, as mentioned, e.g., by Fiedler (1998). A marked influence of the excitation wave form on the control effect on airfoils has indeed been found by, e.g., Amitay & Glezer (2002) and Margalit *et al.* (2005), but the physical mechanism behind is still not fully understood. Konstantinidis & Bouris (2009, 2010) observed that nonharmonic forcing of a cylinder wake with a constant fundamental frequency can excite a wide range of different vortex patterns. Joe *et al.* (2010) numerically determined an optimal wave form in terms of lift increase for the low Reynolds number flow around an inclined flat plate by an adjoint-based approach. The resulting actuation was a "nearly periodic pulsatile forcing at a frequency close to that of the vortex shedding" (Colonius & Williams, 2011).

Traditionally, in an experimental setting, different wave forms are generated by amplitude modulation of the high frequency driving signal of piezoelectric actuators. According

to Wiltse & Glezer (1993), flow nonlinearities demodulate the signal so that only the modulated wave form takes effect and the high frequency content is discarded.

Electromagnetic body forces offer a much more direct way to provide excitation by different wave forms. Indeed, Weier & Gerbeth (2004) and Cierpka *et al.* (2010) found distinct wave form effects in electromagnetically forced flows around airfoils. The attainable lift increment for a fixed angle of attack and a constant excitation frequency at a chord length Reynolds number of around 10^5 scales with the peak rather than the rms value of the momentum input. Consequently, for constant rms momentum, excitation with a triangular wave produced approximately 70% more lift than excitation with a square wave. Similar observations regarding the role of peak and rms momentum input have been reported by Nagib *et al.* (2006) and Naim *et al.* (2007). Stalnov & Seifert (2010) discuss further options for proper scaling of the momentum input in relation to the attainable lift increase.

However, it remains difficult to assign the effects to one of the many flow features on the stalled airfoil. Therefore, we study here the somewhat simpler case of the flow over a backward-facing step with the aim to get a clearer picture. Especially, we aim to answer the question, how the shear layer structures respond to excitation with different wave forms under otherwise identical parameters.

EXPERIMENTAL SETUP AND PARAMETERS

The electromagnetic, i.e., Lorentz force density is generated by an array of magnets and electrodes as sketched in the left part of Fig. 1. Electrodes and permanent magnets are arranged such that their polarity and magnetization direction changes periodically. In that way, a wall parallel Lorentz force density f_L, exponentially decaying with the wall distance, is generated above the actuator. Feeding an alternating current density $j(t)$ into the electrodes generates a Lorentz force oscillating between upstream and downstream direction. Weier & Gerbeth (2004) provide details and further explanation. This actuator has been mounted just in front of the trailing edge of the step.

The force amplitude can be normalized by the free stream momentum resulting in a so called interaction parameter

$$N = \frac{jBa}{\rho U_\infty^2}, \tag{1}$$

where B is the wall normal magnetic induction at the surface of the magnets, a the width of a single electrode or magnet, ρ the fluids' viscosity, and U_∞ the free stream velocity, respectively. N is proportional to the squared ratio of the generated velocity fluctuations to the free stream velocity. In the following, N' denotes the interaction parameter based on the rms value of the electric current.

Particle Image Velocimetry (PIV) measurements have been performed in a free surface electrolyte channel filled with an aqueous sodium hydroxide solution containing 1% NaOH. The test section is 1.2 m long and has a cross section of $0.2\times0.2\,\mathrm{m}^2$. The step height h is 15 mm and the long half-axis of the elliptical nose is mounted 100 mm above the channel floor. This results in an expansion ratio ($1+h/H$, H is the distance from the actuator to the free surface) of 1.16. The aspect ratio of the step is 10.7. Up to now, we have investigated the flow at a step height Reynolds number of 1875.

The PIV setup consists of a 250 mW diode pumped solid state laser with light sheet optics and a Photron Fastcam 1024PCI 100K camera. About 27500 images of 240×1024 pixel were recorded at 125 Hz per parameter configuration and evaluated with PIVview2C 2.4 from PivTec using multigrid interrogation with image deformation and a final window size of 16×16 pixel.

RESULTS AND DISCUSSION

The shear layer spreading rate and the resulting entrainment are directly coupled to the reattachment process: the larger the spreading, the higher the entrainment and the earlier the reattachment (Greenblatt & Wygnanski, 2000). For backward-facing steps, a maximum reduction of the reattachment length x_r is often found for an excitation frequency f_e close to the frequency that is most amplified by the Kelvin-Helmholtz instability of the shear layer (Dandois *et al.*, 2007). To determine the linear stability properties of a flow, it is common practice (see, e.g., Huerre & Rossi, 1998) to investigate the growth or decay of normal modes given by

$$\psi(x,t) = Ae^{i(\alpha x-\omega t)}. \tag{2}$$

A disturbance with a given real frequency ω grows in flow direction x, if its spatial growth rate $-\alpha_i$ is larger than zero. In order to quickly estimate growth rates from experimental data, it is convenient to examine the behavior of naturally present disturbances rather than using consecutive low amplitude excitation with different frequencies. The former method has been suggested and used by Soria & Wu (1992) and later by Khor *et al.* (2011) and boils down to compare the power spectral densities (PSD) at two different downstream locations.

The top part of Fig. 2 shows spatial amplification rates $-\alpha_i$ along the shear layer calculated in this manner from time signals of the y–component of the velocity. The PSD has been estimated at x_0 and x_1. Since the spacing of the PIV grid points (open gray symbols in the bottom part of Fig. 2) is slightly larger than the momentum thickness, the PSD at two different y-positions (blue and orange markers) has been used at x_1. However, given the already considerable scatter of the data points, the differences in terms of growth rate between the locations are minor. θ_m is the characteristic value of the momentum thickness in the middle of the region of exponential growth as introduced by Michalke (1965), and f the frequency. Since the instability characteristics of free and reattaching shear layers are similar (Hasan, 1992), the data show a fair agreement with the calculations of Michalke (1965, 1990) and the measurements of Freymuth (1966) in free shear layers. The higher amplification rates for low frequencies may be connected to the small distance d between shear layer and wall, but might as well be due to oscillations of the reattachment zone. Considering the dint at the higher frequencies, Michalke (1965) remarks related to the experiments by Freymuth (1966) that "for $f\theta_m/U_\infty > 0.1$ the results are doubtful, because exponentially growing disturbances exist only for

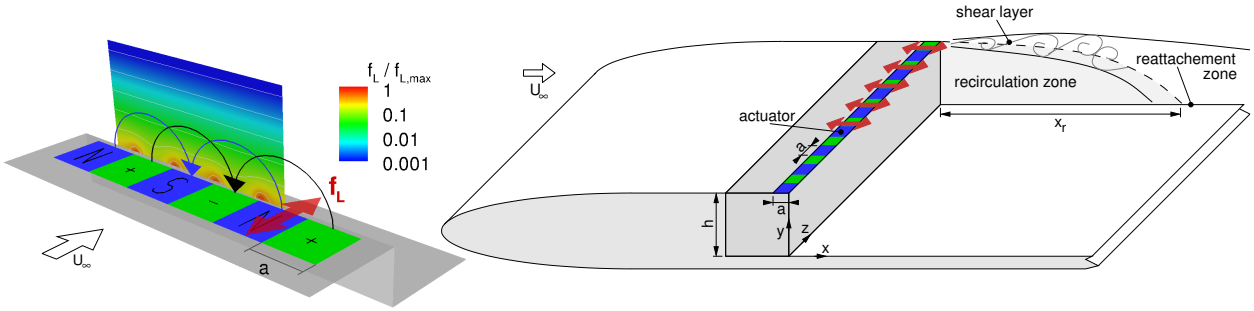

Figure 1. Sketch of the Lorentz force actuator (left) and the backward-facing step (right).

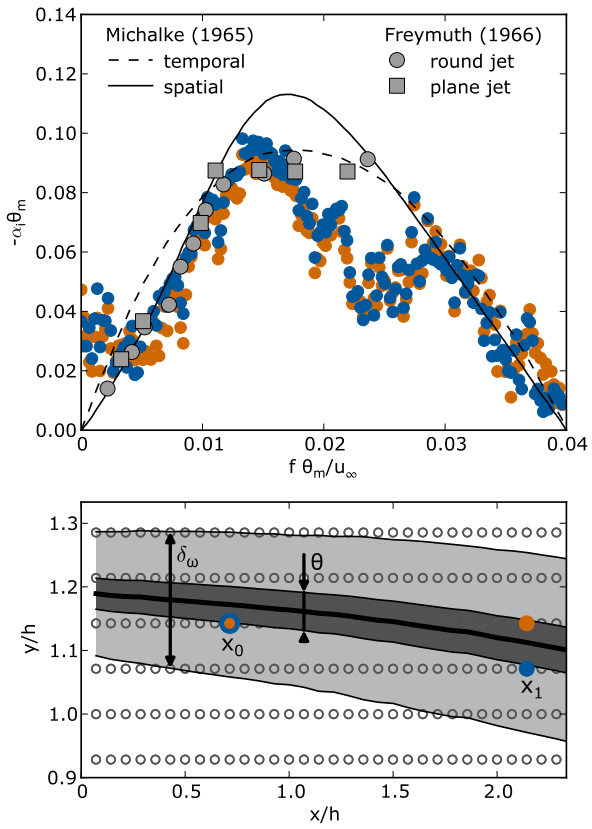

Figure 2. Spatial amplification rates in the shear layer compared to the analytical predictions by Michalke (1965) and the experimental results of Freymuth (1966) (top) determined from power spectral density estimations at the locations in the bottom diagram. Development of the shear layer with downstream location and probe coordinates for the PSD (bottom).

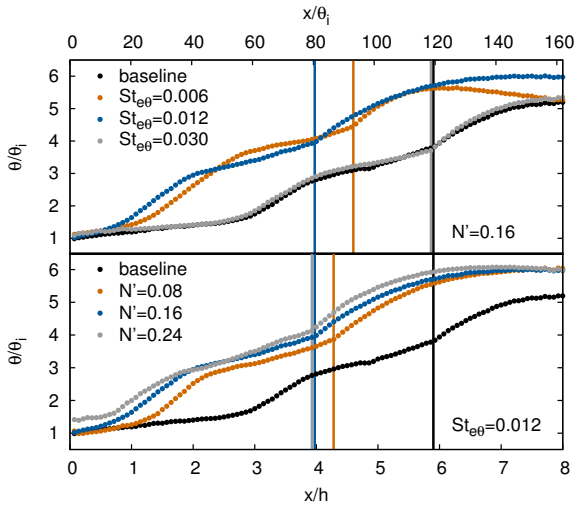

Figure 3. Spatial amplification rates in the shear layer (top) determined from power spectral density estimations at the locations in the bottom diagram.

small values x in the basic flow direction". The growth rate vs. frequency graphs of Khor *et al.* (2011) do indeed show deviations from the theoretical curves similar to that in Fig. 2.

Momentum thickness (θ) growth relative to the initial momentum thickness (θ_i) is depicted in Fig. 3. The unforced shear layer is laminar and therefore grows very slowly initially, but the growth rate increases when the Kelvin-Helmholtz vortices start to roll up ($x > 3\,\mathrm{h}$). The Kelvin-Helmholtz vortices are then convected downstream and, eventually, the shear layer reattaches. Vortex pairing events in the reattached shear layer happen only irregularly and take place on the background of strong three dimensional structures. Forcing at a constant amplitude $N' = 0.16$ leads to a much earlier vortex roll up near the optimal excitation frequency of $St_{e\theta} = f_e\theta_i/U_\infty = 0.012$ and, consequently, x_r is reduced. For the first subharmonic of the optimal excitation frequency, vortex roll up starts later but produces larger vortices. Excitation with the relatively high frequency of $St_{e\theta} = 0.03$ has almost no effect on the flow. Keeping the excitation frequency at $St_{e\theta} = 0.012$ and increasing the forcing amplitude leads to earlier vortex roll up, larger vortices, and shorter reattachment lengths. An interaction parameter of $N' = 0.24$ already changes the mean flow, i.e., the initial momentum thickness.

Figure 4 underlines the above discussion with diagrams of the reattachment length normalized by its value in the unforced flow (x_{r0}) versus N and $St_{e\theta}$, respectively $St_{eh} = f_e h/U_\infty$. Additionally, phase averaged vorticity plots corresponding to the different parameter configurations and the extend of the time averaged recirculation zone are drawn. For the unforced flow, a snapshot of the vorticity distribution and its time average is given instead of a phase average. Forcing with increasing amplitude leads to earlier formation of stronger vortices, and correspondingly shorter reattachment lengths, a process which seemingly approaches saturation for $N' > 0.2$. Observing the reattachment length as a function of excitation frequency reveals again the maximum reduction for

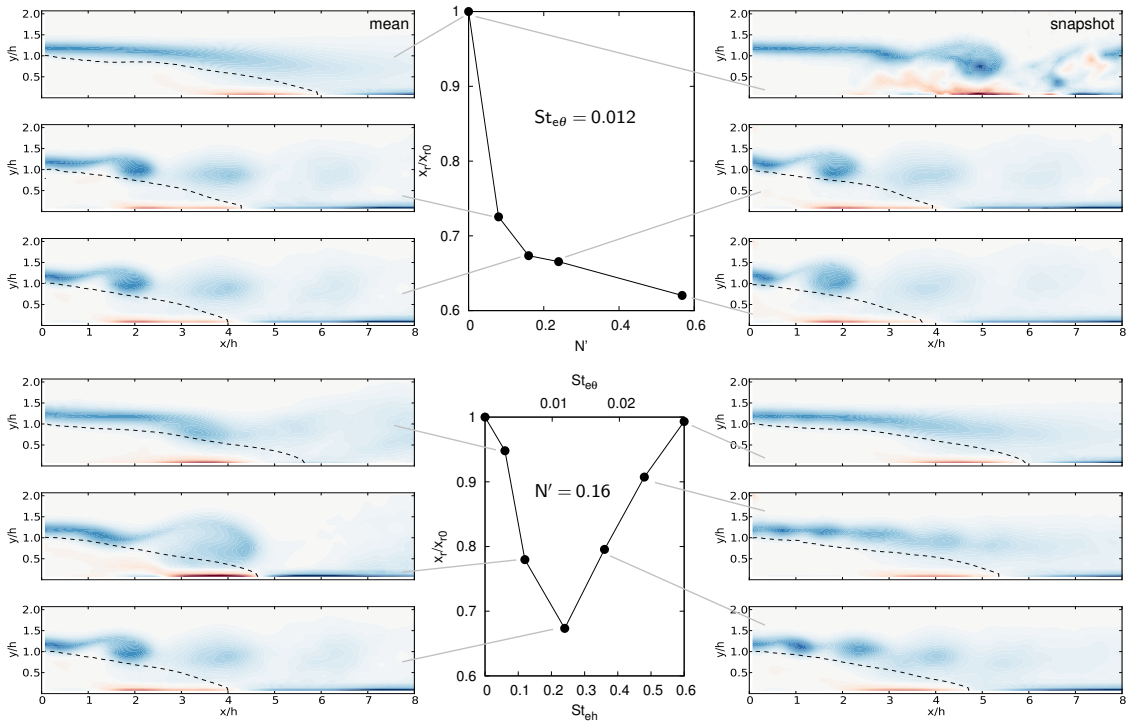

Figure 4. Shortening of the recirculation zone (dashed line) vs. interaction parameter (top) and vs. excitation frequency (bottom) with corresponding plots of phase averaged vorticity.

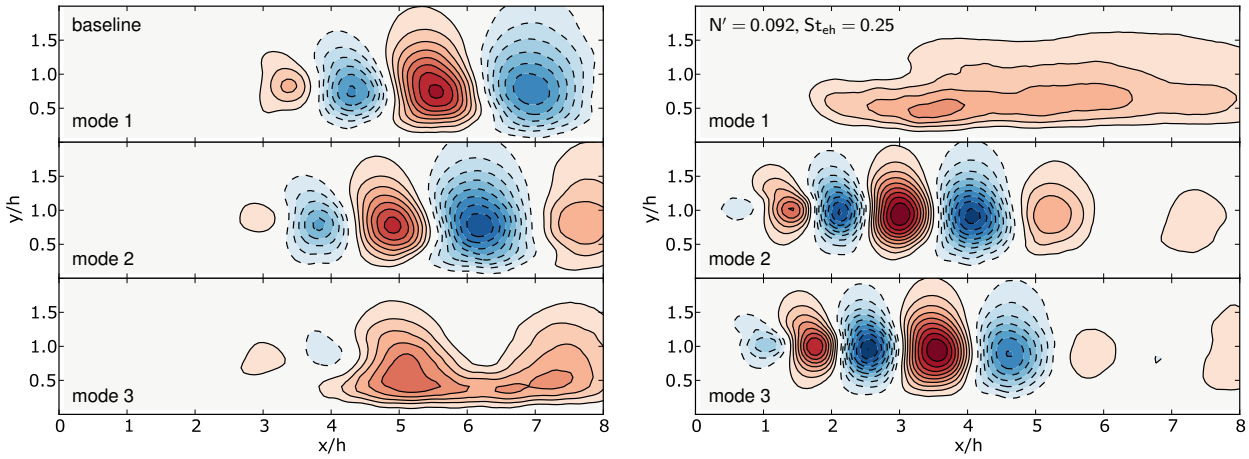

Figure 5. First three POD modes for the baseline flow (left) and the flow under excitation with $N' = 0.092$, $St_{eh} = 0.25$ (right).

$St_{e\theta} = 0.012$. Excitation with frequencies not much lower or higher than this frequency still results in pronounced vortices of larger or smaller size, respectively. If excitation leaves the range of frequencies amplified by the shear layer, the flow no longer responds to the actuation with N'=0.16.

Proper orthogonal decomposition (POD) is often used to extract features from a series of flow realizations $u(\mathbf{x},t)$. It decomposes a flow field into an orthonormal system of spatial modes $\Phi_i(\mathbf{x})$ and corresponding orthogonal temporal coefficients $a_i(t)$:

$$u(\mathbf{x},t) = \sum a_i(t) \cdot \Phi_i(\mathbf{x}). \qquad (3)$$

A gentle introduction and hands on approach can be found in Luchtenburg *et al.* (2009). Normally, and as done in the following, only the fluctuating components of the velocity fields are decomposed. If the decomposition is based on velocity fields, it is optimal in terms of energy. Figure 5 shows the first three POD modes of the y-velocity component for the baseline flow (left) and the flow excited with $N' = 0.092$ at $St_{eh} = 0.25$ (right). In Fig. 6 the modes' relative energy content $\lambda_i / \sum \lambda_i$ is plotted versus the mode number for baseline and excited flow. Figure 7 displays the PSD of the first modes temporal coefficient for both cases. In the baseline case, modes 1 and 2 contain approximately equal energy and show similar

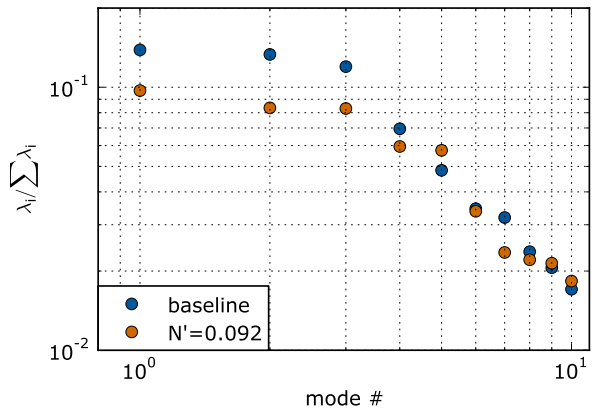

Figure 6. POD spectrum for the baseline and the excited flow, excitation as in Fig. 5.

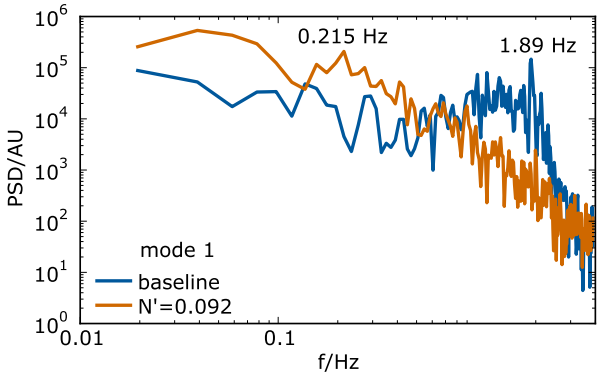

Figure 7. PSD of the temporal coefficient of mode 1 for the baseline and the excited flow, excitation as in Fig. 5.

shape with a phase shift of $\pi/2$. The same holds true for the excited flow modes 2 and 3. It is characteristic for convective structures. Kelvin-Helmholtz vortices appear around $x/h = 3$ for the unforced, but very near the step for the excited flow. Consequently, the modes belonging to these vortices are shifted upstream in case of excitation. Another feature of the exited flows decomposition is a completely different shape of the highest energetic mode, which obviously is not paired. Its maximum is located near the mean reattachment point. Looking at the PSD of its temporal coefficient (Fig. 7), besides the dominant very low frequencies which are mirrored in the $a_i(t)$ of the other modes, one can detect a peak at 0.215 Hz. This peak corresponds quite well to the flapping frequency, which is an expression of the absolute instability of the separated region (see, e.g., Dandois *et al.*, 2007). Mode 3 of the baseline flow shows the signature of this absolute instability as well, albeit with a lower energy content relative to the first and second mode. The 1.89 Hz peak in the spectrum of mode 1 for the baseline flow equals the frequency most amplified by the shear layer, i.e., it is a footprint of the convective instability of the flow. Comparing the POD spectra of the baseline and the excited flow, one finds a lower energy content in the first modes of the latter. This may be a consequence of the earlier reattachment. It leads to strongly fluctuating velocity components in a larger portion of the observed area, which results in

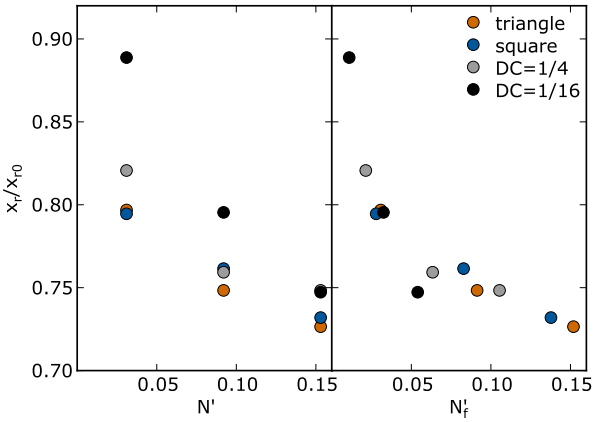

Figure 8. Reattachment length under excitation with $St_{eh} = 0.25$ normalized by the baseline reattachment length vs. rms interaction parameter (N', left part) and vs. N calculated with the rms of the fundamental frequency only (N'_f, right part).

a higher energy content in the higher modes. Additionally, the 2D PIV applied here is unable to capture the inherent three dimensionality in this region of the flow.

Up to now, excitation wave form was always sinusoidal. The effect of other wave forms on reattachment length reductions is shown in Fig 8. In the left part, x_r/x_{r0} is plotted vs. the interaction parameter N' based on the rms value of the applied current. Obviously, different wave forms lead to markedly different reattachment length reductions for a constant N'. Although it is comparing apples to oranges, we observe a trend opposite to what has been found in the case of stalled airfoils. Signals with highest peak to rms momentum ratio perform worst in case of reattachment length reduction, while they were found to be preferable in order to obtain largest lift increments for a given rms momentum input. Plotting the attainable lift increments on the airfoil vs. the peak value of the normalized momentum input collapsed data belonging to different wave forms on a single line (Weier & Gerbeth, 2004). On the contrary, here (i.e., x_r/x_{r0} vs. $\hat{N}$) it would further increase the differences between the wave forms.

To resolve the discrepancy, we have to look at the Fourier series of the excitation wave forms. The excitation frequency in Fig. 8 lies with $St_{eh} = 0.25$ very near the optimum one. For all investigated wave forms, the harmonics have frequencies at least three times higher than the fundamental. These components are beyond the range of frequencies amplified by the shear layer. Therefore, the shear layer can only react on the amplitude of the fundamental sine wave embedded in the different wave forms. Indeed, if we plot x_r/x_{r0} vs. the interaction parameter N'_f calculated with the rms value of *only the fundamental* of the applied wave form, the data are rearranged in such a way that they follow one line in a fair approximation. It goes without saying that we would obtain a similar picture using the peak value of the fundamental.

This implies that looking at the shear layer alone is probably not sufficient to explain the excitation wave form effects observed in the case of stalled airfoils.

CONCLUSION

Electromagnetic excitation of the flow over a backward-facing step has been shown to reduce the reattachment length, provided the shear layer is able to amplify the imposed disturbances. There is an optimal excitation frequency which equals the most amplified frequency of the shear layer instability. Increasing the excitation amplitude at a fixed frequency leads initially to a reduction of the reattachment length, but saturates for higher amplitudes.

While the most energetic modes of the POD of the baseline flow field correspond to the Kelvin-Helmholtz vortices, a POD of the flow under excitation yields under certain conditions to a dominant mode corresponding to the absolute instability (flapping mode) of the separated region.

Using excitation at the most amplified frequency with different wave forms, it is the amplitude of the fundamental that determines the attainable reattachment length reduction.

ACKNOWLEDGMENTS

Financial support from Deutsche Forschungsgemeinschaft in the framework of "SFB 609" is gratefully acknowledged.

REFERENCES

Amitay, M. & Glezer, A. 2002 Controlled transients of flow reattachement over stalled airfoils. *Int. J. Heat Fluid Flow* **23**, 690–699.

Bhattacharjee, S., Scheelke, B. & Troutt, T.R. 1986 Modification of vortex ineractions in a reattaching separated flow. *AIAA J.* **24** (4), 623–629.

Cierpka, C., Weier, T. & Gerbeth, G. 2010 Synchronized force and particle image velocimetry measurements on a NACA 0015 in poststall under control of time periodic electromagnetic forcing. *Phys. Fluids* **22** (7), 075109.

Colonius, T. & Williams, D.R. 2011 Control of vortex shedding on two- and three-dimensional aerofoils. *Phil. Trans. R. Soc. A* **369** (1940), 1525–1539.

Dandois, J., Garnier, E. & Sagaut, P. 2007 Numerical simulation of active separation control by a synthetic jet. *J. Fluid Mech.* **574**, 25–58.

Eaton, J.K. & Johnston, J.P. 1981 A review of research on subsonic turbulent flow reattachment. *AIAA J.* **19** (9), 1093–1100.

Fiedler, H. 1998 Control of free turbulent shear flows. In *Flow Control* (ed. M. Gad-el Hak & A. Pollard), *Lecture Notes in Physics monographs*, vol. 53, pp. 335–429. Springer Berlin / Heidelberg.

Freymuth, P. 1966 On transition in a separated laminar boundary layer. *J. Fluid Mech.* **25** (4), 683–704.

Greenblatt, D. & Wygnanski, I. 2000 The control of flow separation by periodic excitation. *Prog. Aero. Sci.* **36**, 487–545.

Hasan, M.A.Z. 1992 The flow over a backward-facing step under controlled perturbation: laminar separation. *J. Fluid Mech.* **238**, 73–96.

Huerre, P. & Rossi, M. 1998 Hydrodynamic instabilities in open flows. In *Hydrodynamic and Nonlinear Instabilities* (ed. C. Godréche & P. Manneville), chap. 2, pp. 81–294. Cambridge University Press.

Huppertz, A. 2001 Aktive Beeinflussung der Strömung stromab einer rückwärtsgewandten Stufe. PhD thesis, TU Berlin.

Joe, W.T., Colonius, T. & MacMynowski, D.G. 2010 Optimized waveforms for feedback control of vortex shedding. In *Active Flow Control II* (ed. R. King), *Notes on Numerical Fluid Mechanics and Multidisciplinary Design*, vol. 108, pp. 391–404. Berlin: Springer.

Khor, M., Sheridan, J. & Hourigan, K. 2011 Power-spectral density estimate of the Bloor-Gerrard instability in flows around circular cylinders. *Exp. Fluids* **50**, 527–534.

Konstantinidis, E. & Bouris, D. 2009 Effect of nonharmonic forcing on bluff-body vortex dynamics. *Phys. Rev. E* **79**, 045303.

Konstantinidis, E. & Bouris, D. 2010 The effect of nonharmonic forcing on bluff-body aerodynamics at a low Reynolds number. *J. Wind Eng. Ind. Aerodyn.* **98**, 245–252.

Luchtenburg, D.M., Noack, B.R. & Schlegel, M. 2009 An introdution to the POD Galerkin method for fluid flows with analytical examples and MATLAB source codes. *Tech. Rep.* 01. Berlin Institute of Technology MB1, Müller-Breslau-Str. 11, D-10623 Berlin.

Margalit, S., Greenblatt, D., Seifert, A. & Wygnanski, I. 2005 Delta wing stall and roll control using segmented piezoelectric fluidic actuators. *J. Aircraft* **42** (3), 698–709.

Michalke, A. 1965 On spatially growing disturbances in an inviscid shear layer. *J. Fluid Mech.* **23** (3), 521–544.

Michalke, A. 1990 On the inviscid instability of wall-bounded velocity profiles close to separation. *Z. Flugwiss. Weltraumforsch.* **14**, 24–31.

Nagib, Hassan, Kiedaisch, John, Reinhard, Paul & Demanett, Brian 2006 Control techniques for flows with large separated regions: A new look at scaling parameters. AIAA–paper 2006-2857.

Naim, A., Greenblatt, D., Seifert, A. & Wygnanski, I. 2007 Active control of a circular cylinder flow at transitional reynolds numbers. *Flow, Turbulence and Combustion* **78** (3–4), 383–407.

Roos, F.W. & Kegelmann, J.T. 1986 Control of coherent structures in reattaching laminar and turbulent shear layers. *AIAA J.* **24** (12), 1956–1963.

Soria, J. & Wu, J. 1992 The character of the instability of the separated shear layer from a square leading edge flat plate. In *11^{th} Australasian Fluid Mechanics Conference*, pp. 391–394. University of Tasmania, Hobart, Australia.

Stalnov, O. & Seifert, A. 2010 On amplitude scaling of active separation control. In *Active Flow Control II* (ed. R. King), *Notes on Numerical Fluid Mechanics and Multidisciplinary Design*, vol. 108, pp. 63–80. Berlin: Springer.

Weier, T. & Gerbeth, G. 2004 Control of separated flows by time periodic Lorentz forces. *Eur. J. Mech. B/Fluids* **23**, 835–849.

Wiltse, J.M. & Glezer, A. 1993 Manipulation of free shear flows using piezoelectric actuators. *J. Fluid Mech.* **249**, 261–285.